Quantitative Detection of Rheumatic Heart Disease from 2D Echocardiography

Alexander Clark; Arian Khorshid; Scott Muffly; Craig Sable, MD; Andrea Beaton, MD; Paul Matherne, MD; Jeffrey Holmes, MD, PhD

Abstract

Rheumatic heart disease (RHD) continues to pose a heavy burden in many developing countries. Limited medical resources, shortage of medical personnel, and time-intensive screening methods have prevented a substantial mitigation of this burden. Despite the recent determination of evidence-based guidelines for diagnosis of RHD via echocardiography, a fast, accurate means by which large populations of patients at risk for RHD can be screened has not been developed yet. Here we demonstrate a novel semi-automatic computer algorithm that incorporates quantitative criteria from the World Heart Federation's (WHF) evidence-based guidelines to quickly screen echocardiograms for certain morphological and hemodynamic signs of RHD. The algorithm consists of two parts. The first generates a tracing of the anterior mitral valve leaflet (AMVL) with a novel gradient border detection algorithm (GBAD) and snake function. The second quantifies the extent of mitral regurgitation by image filtering and shape recognition. The AMVL tracing algorithm generated an adequate tracing of the AMVL 53% of the time. Evaluation of the semi-automated mitral regurgitation algorithm using an image set (n=49) of known diagnoses yielded a sensitivity of 97% and a specificity of 100%.

Introduction

RHD kills hundreds of thousands annually and is the most common acquired heart disease found among children and young people in developing countries (Carapetis et al., 2005). It is estimated to afflict nearly 15 million people annually, and its incidence is increasing (Carapetis et al., 2005). While virtually eradicated in the developed world, RHD persists in developing countries due to a lack of widely available screening among susceptible populations (Figure 1). Until recently, RHD was primarily diagnosed by auscultation for heart murmurs, but newer studies, relying on echocardiography to enhance the diagnosis of RHD, have shown that subclinical endocarditis exists at rates up to 10 times higher than that diagnosed by auscultation alone (Carapetis et al., 2008). Recognition of subclinical endocarditis can identify patients who would benefit from secondary antibiotic prophylaxis and hopefully prevent the progression to clinically significant RHD (Seckeler and Hoke, 2011).

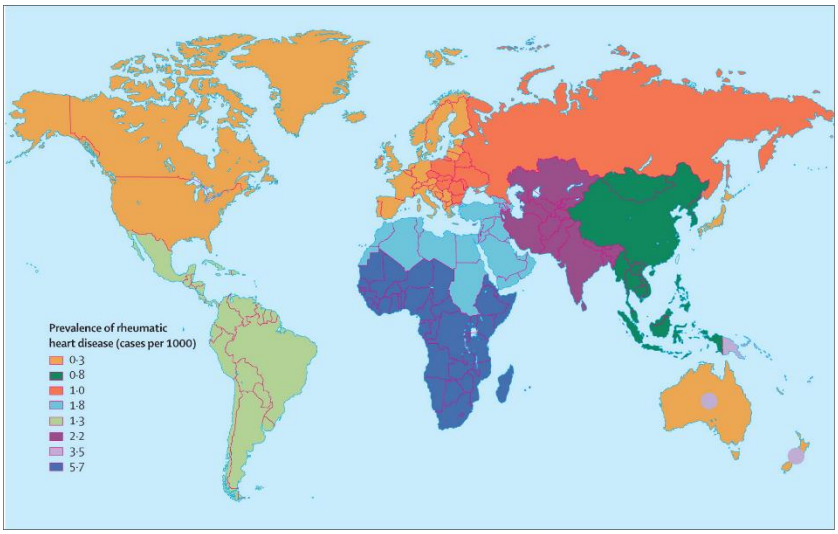

Figure 1. Global prevalence of rheumatic heart disease. *Source: Lancet Infect Dis. 2005;5:685-694*

The pathogenesis of RHD originates from a *Streptococcus pyogenes* infection (Guilherme et al., 2007). The improper treatment of this infection with antibiotics makes subjects particularly susceptible to an autoimmune

Table 1. Morphological Criteria
Definite RHD (either A, B, C, or D):
A) Pathological MR and at least two morphological features of RHD of the MV
B) MS mean gradient ≥4 mmHg
C) Pathological AR and at least two morphological features of RHD of the AV
D) Borderline disease of both the AV and MV
Borderline RHD (either A, B, or C):
A) At least two morphological features of RHD of the MV without pathological MR or MS
B) Pathological MR
C) Pathological AR
Normal echocardiographic findings (all of A, B, C, and D):
A) MR that does not meet all four Doppler echocardiographic criteria (physiological MR)
B) AR that does not meet all four Doppler echocardiographic criteria (physiological AR) C) An isolated morphological feature of RHD of the MV (for example, valvular thickening) without any associated pathological stenosis or regurgitation D) Morphological feature of RHD of the AV (for example, valvular thickening) without any associated pathological stenosis or regurgitation

Table 2. Hemodynamic Criteria
Pathological mitral regurgitation*
Seen in two views
In at least one view, jet length ≥2 cm[1]
Velocity ≥3 m/s for one complete envelope
Pan-systolic jet in at least one envelope
Pathological aortic regurgitation*
Seen in two views
In at least one view, jet length ≥1 cm[1]
Velocity ≥3 m/s in early diastole
Pan-diastolic jet in at least one envelope
*All four Doppler echocardiographic criteria must be met; [1]Jet length measured from vena contracta to last pixel of regurgitant color

response characterized by rheumatic fever (RF). There are also indications that genetic and environmental factors influence susceptibility. Of children afflicted with RF, 30-45% develop carditis, which causes damage to heart valves. The morphological and hemodynamic abnormalities resulting from chronically untreated RF progresses to RHD and, eventually, to heart failure. Of particular significance to the rationale behind this study is that RF is completely preventable by administration of antibiotics, such as penicillin, during the preceding streptococcal infection.

In February 2012, the WHF released the first evidence-based guidelines for detection of RHD by 2D echocardiography (Reményi et al., 2012). These guidelines provide promising criteria by which to quantitatively screen for RHD (Tables 1, 2). Screening performed by this method would be advantageous in three ways. First, it would reduce the interobserver variability likely

associated with current, qualitative RHD screening standards of auscultation and manual interpretation of echocardiograms by a cardiologist. Second, use of standardized, objective detection criteria would allow for some degree of automation of the screening process, which could potentially reduce screening time and increase the accessibility of RHD screening. Lastly, widespread population screening would ease the diagnostic burden on limited medical personnel by eliminating from the treatment pool those individuals who do not exhibit any signs of subclinical RHD.

We have developed a semi-automated detection algorithm to analyze 2D echocardiography for quantitative identification of RHD. The algorithm is composed of two components that assess morphological and hemodynamic abnormalities associated with RHD. The first component uses a novel border detection algorithm and a preexisting snake algorithm (Kass et al., 1988) to trace the anterior mitral valve leaflet. This trace allows for identification of various morphological criteria, as defined by WHF, for diagnosis of RHD. The second component incorporates a series of filtering steps followed by shape detection to identify and measure the length of a mitral regurgitation jet during systole. Together, these components categorize each patient as either normal or exhibiting subclinical signs of RHD. This screening is meant to complement current efforts by focusing diagnostic and treatment resources on populations most at risk for developing chronic, clinical RHD.

Methods

Patient Dataset

The de-identified dataset that was analyzed was acquired from collaborators at Children's National Medical Center from a screening study of Ugandan children (Beaton et al., 2012). All of the images had been assessed by a cardiologist using the WHF guidelines and the patients had been classified as normal, borderline or abnormal. This diagnosis and the cardiologist's measure of the length of the maximum mitral regurgitant jet for each patient are the outputs that the program is tested against.

The dataset consists of 49 independent parasternal long echo image stacks. Of the 49 patients, 10 had been diagnosed as normal (no subclinical indications of RHD) and the remaining 39 as borderline and abnormal (some degree of subclinical RHD). Analysis of the AMVL tracing algorithm used a random selection of 17 of these image stacks. For analysis of the mitral regurgitation detection algorithm, a single image was manually chosen from each of the 49 image stacks based on the presence and severity of the mitral regurgitant jet.

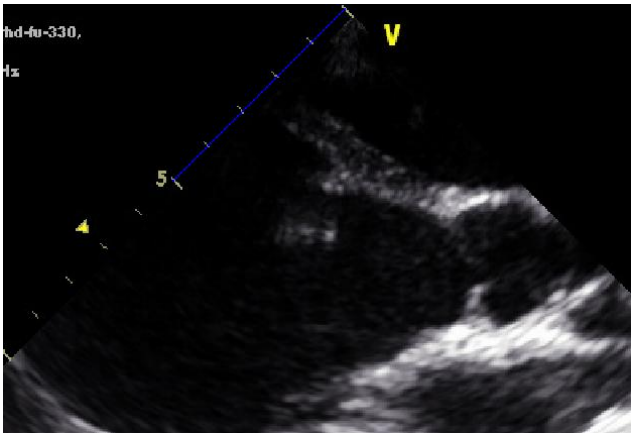

Figure 2. The scale bar present on the echo image was used to create a pixel-to-centimeter conversion method.

WHF guidelines

The WHF guidelines for detection of RHD include both morphological and hemodynamic factors (Reményi et al., 2012). The morphological changes that occur include thickening of the mitral valve, restricted and

excessive motions of the mitral and aortic valves, and coaptation defects in the mitral and aortic valves. Coaptation defects are characterized by improper closing of the valve and are often a result of excessive leaflet motion. Restricted leaflet motion is often a result of leaflet thickening and can cause regurgitation. The hemodynamic considerations include pan-systolic mitral and aortic regurgitation. The length of these regurgitant jets can be measured using Doppler echocardiography technology.

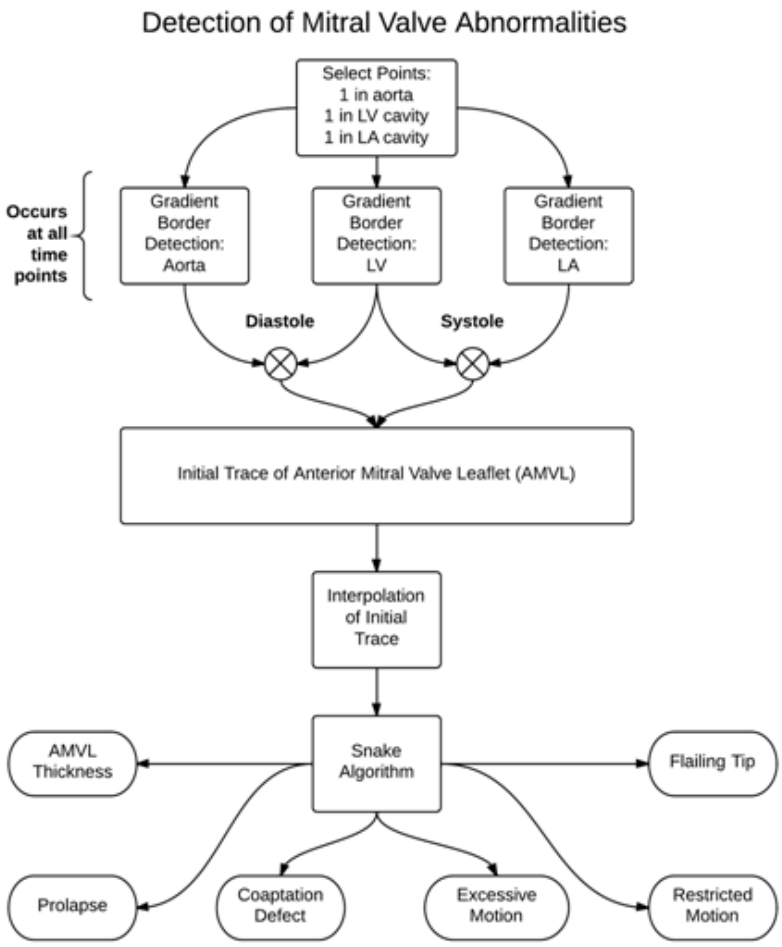

Figure 3. Overview of the process to detect mitral valve morphological abnormalities indicative of RHD.

Pixel to Centimeter Conversion

A pixel to centimeter conversion algorithm was developed for interpretation of the measured regurgitant jet. Although this data is usually included within the image dataset, it is often lost during the de-identification process. The edge of each echocardiogram has a scale bar (Figure 2). The method searches for the contact point of the transducer, the vertex at the top of the echo. Once this point is found, a line follows the left edge of the projected image. The projection forms a 90° angle at the center of the image slice with the pixel intensities outside the projection equal to zero. The line following this projection will eventually hit the first scale bar (pixel intensity > 0), which corresponds to 5 cm. This method provides a means of converting between pixels and centimeters, which is necessary when measuring mitral leaflet thickening, mitral leaflet excursion, mitral valve prolapse, and the length of the regurgitant jet.

Border Detection Algorithms

Border detection algorithms provide the basis for measurement of morphological abnormalities. Most abnormalities can be viewed with the greatest clearly in the parasternal long axis view. Other views, such as parasternal and apical short axes, are typically used to reinforce the observations made from the parasternal long axis view. The morphological changes that can be detected include mitral leaflet thickening and excessive leaflet motion. The objective criteria for detection of these changes is covered in detail in the WHF guidelines (Reményi et al., 2012). Some of the criteria, such as aortic leaflet thickening, are subjective and lack quantitative metrics

for analysis. As such, these morphological abnormalities were excluded from the program's analysis.

The semi-automated detection of the mitral valve throughout the cardiac cycle requires precise and consistent tracing of the mitral leaflet border. The algorithm includes a series of methods to provide a tracing for each image frame. These methods include a gradient border detection algorithm (GBAD) to get a rough estimate of the mitral leaflet position, an interpolation to uniformly distribute points close to the mitral valve leaflet, and finally a snake algorithm that places points on the border of the traced leaflet (Figure 3).

Gradient Border Detection Algorithm

The gradient border detection algorithm is a custom MATLAB based program which relies on the user to select three landmarks on the image: left ventricular cavity, left atrial cavity, and aortic root (Figure 4A). A polar array of 360 points moves radially outward from each of the landmarks. These points progress until a pixel intensity of 60 or until a 20x20 pixel block average intensity of less than 0.1 is found. Thus, there is a dataset of points associated with each of the landmarks. Typically, pixel intensity in the cavity is not more than 60, so the border detection is straightforward. The 20x20 pixel block of approximately zero intensity indicates a point that is outside of the echo. This was necessary to account for, as the parasternal long axis view cuts off the apex causing points to migrate out of the echo. A subset of points that best contours the AMVL is manually selected from each of the landmark datasets. These points are combined into one dataset that fits the AMVL and is used as an input into the snake algorithm (Figure 4B).

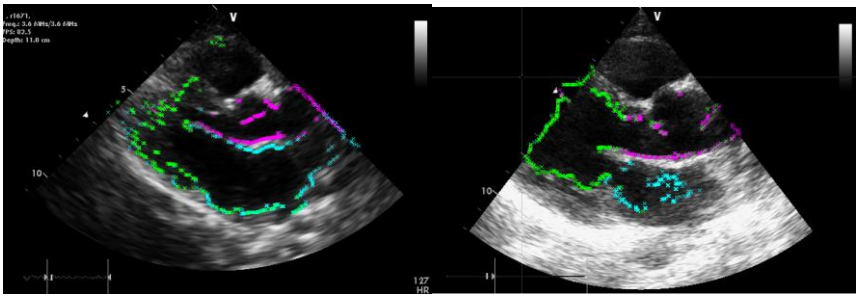

Figure 4. Examples of appropriate (A) and inappropriate (B) tracings of the AMVL.

The ability of GBAD to find the AMVL was evaluated. This was necessary to determine whether the tracing was appropriate for input into the snake algorithm. Appropriate input required the tracing to cover the entire AMVL with no interruptions (**Figure 5 - good v. bad tracing...Alex, you'll have to make this figure since you have the screenshots**). This is a conservative criteria for input, as the entire AMVL does not need to be traced to find the thickness near the tip. Parasternal long axis image sets from 17 randomly selected patients were analyzed using GBAD.

Smoothing AMVL Trace

In order to get a smoother trace of the mitral leaflet border the MATLAB robust loess smooth method is used to interpolate the mitral leaflet points from GBAD (Figure 7A). Points are then moved 5 pixels away from the border, perpendicular to the interpolated dataset. This ensures the input dataset for the snake algorithm does not have any points inside the AMVL wall since the algorithm requires the points to all be on the same side of the wall.

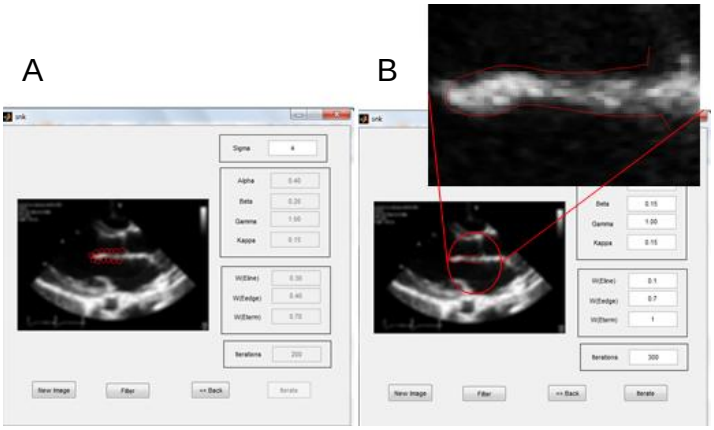

Figure 7. The robust loess smooth method (A) produces appropriate input for the snake method. Use of the snake (B) function from MATLAB Central generates a smooth trace of the AMVL.

The data from the smoothing algorithm is inputed into a snake algorithm (Kass et al., 1988) from MATLAB Central developed by Ritwik Kumar. The snake algorithm requires 15-20 points adjacent to the mitral leaflet. The algorithm uses an energy minimization function with preset parameters to converge on the AMVL outline (Figure 7). The final trace of the leaflet can be used to determine the thickness of the AMVL, providing another quantitative measure for detecting RHD.

Mitral Regurgitation

An algorithm has been developed to determine the extent of regurgitation through the mitral valve during systole. A user first selects a frame during systole, then the program finds and measures the length of the jet. This algorithm requires the three points that were selected for GBAD. A series of filtering methods are used before the regurgitant jet can be found. Once found, an ellipse is fit to the jet, and the long axis of this jet is taken to be the length of the jet.

Filtering

Filtering begins by decreasing the image to 80% of its original size (Figure 8A). This does not remove the region of the image with the regurgitant jet. The purpose is to limit the space that the algorithm must search within in order to minimize computation time.

The first filtering method used removes grayscale pixels from the image frame (Figure 8B). This is done by removing any pixels with RGB values within the same 30 pixel intensity range. Consequently, anatomical components in the background are also filtered out. Following this, the red pixels are deleted from the frame (Figure 8C), because they indicate flow that is moving towards the transducer, and based on the position of the parasternal long axis view, the regurgitant jet is always moving away. The method zeroes all pixels with red values greater than the sum of the green and blue values.

Following the color filtering, MATLAB's built-in bwconncomp function locates all of the remaining groups of pixels. The groups that are below 25 mm^2 are removed because regurgitation caused by RHD has an area greater than 25 mm^2 (Figure 8D). The remaining groups are fitted with an ellipse using MATLAB's built-in regionprops function (Figure 8E).

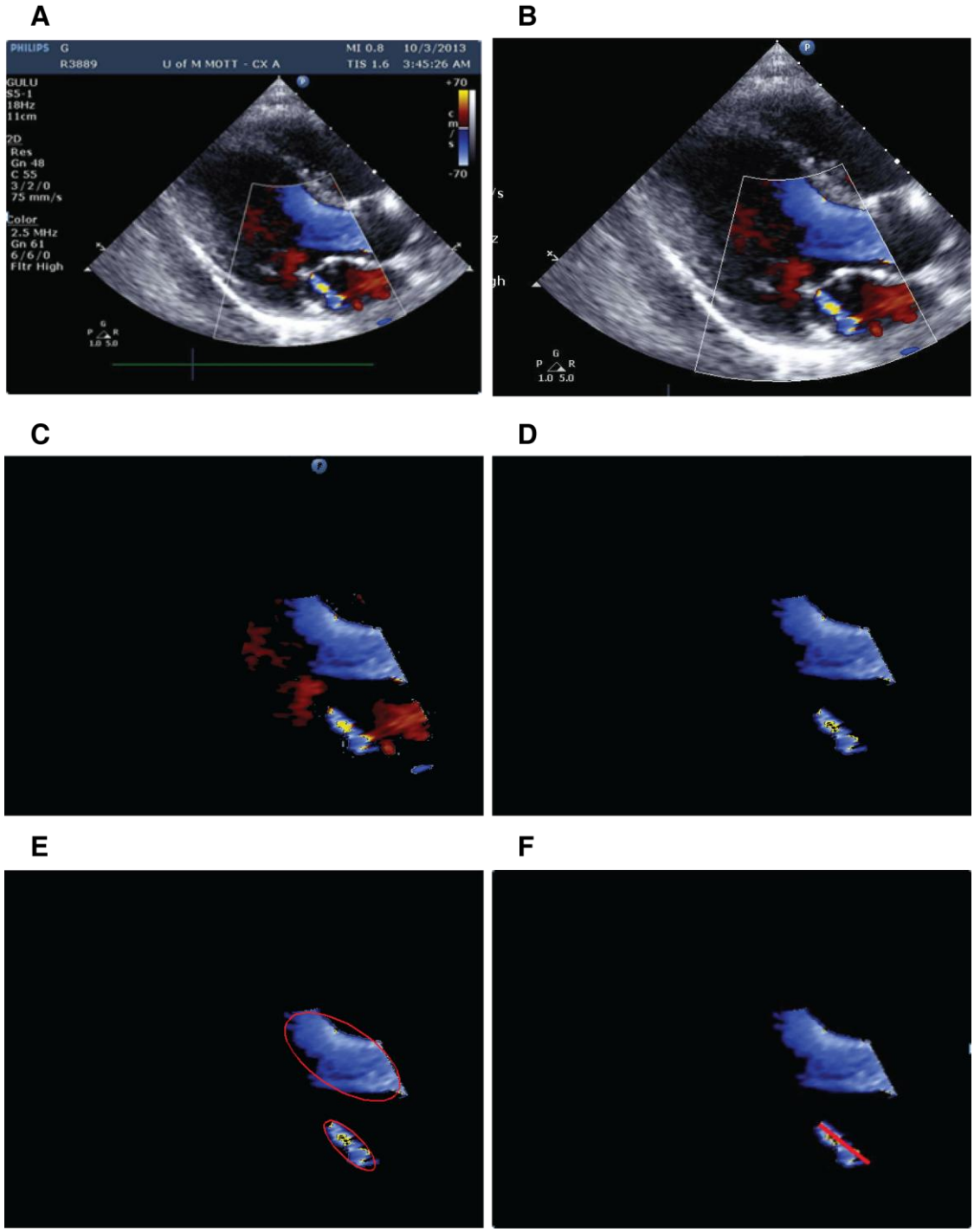

Figure 8. A filtering sequence was used to identify and measure the mitral regurgitation jet. The raw image (A) was first cropped to 80% of its original size to show only the transducer field of view (B). Next, white was filtered out (C), then red (D), followed by envelopment of blue groups above a certain size threshold (E). Finally, the regurgitant jet was identified and the long axis of its corresponding envelope measured (F).

Groups that are traced with an ellipse are then filtered based on the direction of the jet. The angle of the long axis of the jet is usually between 0 and -90 degrees. All jets with angles outside of that range are ignored. Next the average of the three points that were selected for GBAD is located. The program then locates the ellipse with a centroid point that is both closest to and

below the average of the three points. The group of pixels outlined by this ellipse is defined as the regurgitant jet. If there are no ellipses with a centroid below the average point, the program considers that patient to not have mitral regurgitation. The long axis of the ellipse is taken to be the length of the regurgitant jet (Figure 8F).

In addition to the algorithm above, a different program has also been developed that does not use the average of the three points from GBAD. If there are ellipses that remain after all of the filtering (color, size, angle), it then selects the ellipse that is furthest from the transducer. The reason this ellipse is selected is because the aortic outflow can be confused as the regurgitant jet, but is always closer to the transducer. This performance of this fully automated version was compared to the performance of the semi-automated version.

Results

AMVL tracing

The AMVL tracing method was evaluated to determine its effectiveness in generating an adequate trace of the AMVL. This is necessary for the snake algorithm to operate properly. GBAD found the AMVL in 53% of patients. However, a portion of the tip of the AMVL was found in all of the patients (Figure 4A, B). Further testing needs to be done to determine if tracing of just the tip is enough to find the thickness of the AMVL.

MR quantification

The sample image dataset of 49 patients was then used to test the accuracy of the mitral regurgitation algorithm by comparing it to the cardiologist's diagnosis. This assessment was performed twice - once each for semi-automated and fully automated versions of the algorithm - to determine if the degree of automation affected the performance of the algorithm. The sensitivity and specificity of both versions of the algorithm were then calculated (Figure 10). The semi-automated version of the program resulted in an increase in both sensitivity and specificity compared to the automated version. While the change in sensitivity between the automated and semi-automated versions was not very marked (94% and 97%, respectively), a pronounced increase in specificity was observed. Compared to the fully automated version of the algorithm, the semi-automated version exhibited a 60% increase in specificity (from 40% to 100%).

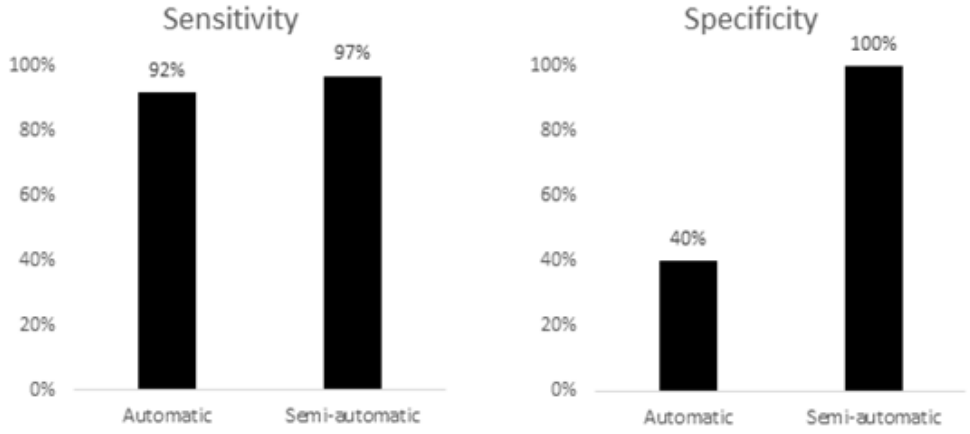

Figure 10. Comparison of sensitivity and specificity between semi-automated and fully automated versions of the algorithm.

Discussion

The novel RHD detection method presented here is, to our knowledge, the first attempt to incorporate the recent WHF criteria for diagnosis of RHD into a semi-automated software detection package. Compared to auscultation, our software provides a much more sensitive screening method for detection of subclinical RHD. Chronic, clinical RHD is a completely preventable condition when secondary prophylaxis of antibiotics is properly administered during the subclinical stage of the disease. In conjunction with echocardiography, the presented software is capable of detecting subclinical RHD earlier than current screenings protocols for three reasons: it is more sensitive compared to auscultation alone (Roberts et al., 2013); it is more accessible because it does not require the interpretation of a cardiologist; and it is more portable because it can be used in conjunction with handheld ultrasound devices. Our software aims to find, from amongst the most at-risk population of children and adolescents, those who do not exhibit any symptoms of subclinical RHD, so that further screening and treatment efforts can be focused on those showing symptoms.

Previous subclinical RHD research has required physicians to diagnose patients based on the quantitative and qualitative WHF criteria. Although physician diagnosis is the gold standard for diagnosing RHD, it is not possible to implement widespread screenings in the countries most affected by the disease. We approached this problem by developing a novel software that eases the burden of diagnosis on physicians by shifting it to a community health worker operating the semi-automated detection program. Since the semi-automated program requires little technical or physiological expertise, community health workers can be trained to operate it. The fully automated method does not filter out enough of the normal patients to relieve enough of the burden off of physicians. However, the performance of the semi-automated method indicates it could be used as a potential replacement for physician diagnosis in resource-limited circumstances.

Conclusion

The results from this study indicate that our novel RHD detection software can be used to improve the diagnostic efficiency of RHD in the developing world. Comparison of the performance of the mitral regurgitation detection software with known physician diagnoses shows promise for introducing a computer-generated diagnostic of subclinical RHD. Although the AMVL tracing software was not compared to physician measurements, the ability to find the outline of the AMVL is also promising for getting an accurate semi-automated thickness measure. In combination, these two methods may be used to decrease the burden of RHD diagnosis on physicians.

Supplementary Algorithms

Tracking the Cardiac Cycle

This method automates the detection of where each image frame is in the cardiac cycle. All of the echocardiography images have an ECG readout located in the bottom left corner of the image. The ECG readout includes a white line indicating where the current view is in relation to the cardiac cycle. In order to assign different portions of the cardiac cycle to different portions of the ECG readout line, first the top of the QRS complex is found. This is accomplished by finding the maximum y-coordinate along the line. From there, the Q and S are the left and right local y-coordinate minimums. The P and T coordinates are the next left and right local y-

coordinate maximums. By finding the P wave, QRS complex and T wave and the white bar indicating the time in the cardiac cycle, a rough idea of where each frame is in the cardiac cycle can be determined. This aids in determining the extent of mitral leaflet motion throughout the cardiac cycle. Both too much and too little mitral leaflet motion are indicative of RHD (Reményi et al., 2012). This necessitates the inclusion of a three-lead ECG readout as part of the echocardiographic system.

References

Beaton, A., Okello, E., Lwabi, P., Mondo, C., McCarter, R., and Sable, C. (2012). Echocardiography screening for rheumatic heart disease in Ugandan schoolchildren. Circulation *125*, 3127–3132.

Carapetis, J.R., Steer, A.C., Mulholland, E.K., and Weber, M. (2005). The global burden of group A streptococcal diseases. Lancet Infect. Dis. *5*, 685–694.

Carapetis, J.R., Hardy, M., Fakakovikaetau, T., Taib, R., Wilkinson, L., Penny, D.J., and Steer, A.C. (2008). Evaluation of a screening protocol using auscultation and portable echocardiography to detect asymptomatic rheumatic heart disease in Tongan schoolchildren. Nat. Clin. Pract. Cardiovasc. Med. *5*, 411–417.

Guilherme, L., Ramasawmy, R., and Kalil, J. (2007). Rheumatic Fever and Rheumatic Heart Disease: Genetics and Pathogenesis. Scand. J. Immunol. *66*, 199–207.

Kass, M., Witkin, A., and Terzopoulos, D. (1988). Snakes: Active contour models. Int. J. Comput. Vis. *1*, 321–331.

Reményi, B., Wilson, N., Steer, A., Ferreira, B., Kado, J., Kumar, K., Lawrenson, J., Maguire, G., Marijon, E., Mirabel, M., et al. (2012). World Heart Federation criteria for echocardiographic diagnosis of rheumatic heart disease--an evidence-based guideline. Nat. Rev. Cardiol. *9*, 297–309.

Roberts, K.V., Brown, A.D.H., Maguire, G.P., Atkinson, D.N., and Carapetis, J.R. (2013). Utility of auscultatory screening for detecting rheumatic heart disease in high-risk children in Australia's Northern Territory. Med. J. Aust. *199*, 196–199.

Seckeler, M.D., and Hoke, T.R. (2011). The worldwide epidemiology of acute rheumatic fever and rheumatic heart disease. Clin. Epidemiol. *3*, 67–84.